High-temperature quantum oscillations of a nonequilibrium non-Fermi liquid

Oles Matsyshyn [1], Li-kun Shi [2], and Inti Sodemann Villadiego [3]
[1] *Division of Physics and Applied Physics, School of Physical and Mathematical Sciences, Nanyang Technological University, Singapore 637371, Singapore*
[2] *Center for Quantum Matter, School of Physics, Zhejiang University, Hangzhou 310058, China*
[3] *Institut für Theoretische Physik, Universität Leipzig, Brüderstraße 16, 04103 Leipzig, Germany*

(Received 6 January 2026; revised 29 June 2026; accepted 1 July 2026; published 10 August 2026)

A periodically driven Fermi gas coupled to a simple boson bath reaches a nonequilibrium steady-state occupation with sharp nonanalyticities at certain momenta. Here, we demonstrate that these nonanalyticities behave as emergent Fermi surfaces by showing that they give rise to quantum oscillations of observables with a period controlled by the effective Fermi-surface area enclosed by these nonanalyticities. However, these oscillations have several striking differences with standard equilibrium quantum oscillations. For example, they remain nonanalytic at finite temperatures, their amplitude can survive up to extremely high temperatures comparable to the frequency of the drive, and they can display nonmonotonic temperature dependence completely at odds with standard Lifshitz-Kosevich behavior.

DOI: 10.1103/pmsn-5jtp

I. INTRODUCTION

The Fermi surface is typically viewed as a characteristic of equilibrium Fermi liquids which is sharp only at zero temperature. However, recent studies have demonstrated that the steady-state occupations of periodically driven Fermions can display nonanalyticities that behave as emergent Fermi surfaces [1–3]. In particular, fermions driven periodically with a frequency Ω (e.g., by monochromatic light) and coupled to a local bosonic ohmic bath, display a jump of the second derivative at wave vector $k_F^2/2m = \hbar\Omega$ [3] (see Fig. 1), which remains sharp even when the bath is at finite temperature and gives rise to phenomena reminiscent of those of equilibrium non-Fermi liquids [3].

In this study, we will demonstrate that these nonanalyticities behave as emergent Fermi surfaces by showing that they give rise to quantum oscillations in response to magnetic fields with a period controlled by their enclosed area in momentum space. However, we will show that many of their properties differ sharply from those of equilibrium Fermi liquids, further substantiating the idea that they behave as the Fermi surface of a nonequilibrium non-Fermi-liquid state. For example, we will demonstrate that, amazingly, the quantum oscillations of these nonequilibrium states are nonanalytic as a function of magnetic field even at finite temperature, and that their amplitude is a nonmonotonic function of temperature that can survive up to extremely high temperatures comparable to the driving frequency, which is completely at odds with equilibrium behavior [4].

II. PERIODICALLY DRIVEN FERMIONS COUPLED TO A BOSON BATH

We consider a system of fermions driven by a time-periodic Hamiltonian $\hat{H}_{\rm e}(t) = \hat{H}_{\rm e}(t+T)$. This system is coupled via $\hat{H}_{\text{e-b}}$ to a bosonic bath governed by $\hat{H}_{\rm b}$, yielding the total Hamiltonian

$$\hat{H}(t) = \hat{H}_{\rm e}(t) + \hat{H}_{\rm b} + \hat{H}_{\text{e-b}}, \tag{1}$$

where $\hat{H}_{\rm e}(t) = \sum_{\alpha\beta} \langle\alpha|\hat{h}_t|\beta\rangle \hat{c}_\alpha^\dagger \hat{c}_\beta$, $\hat{H}_{\rm b} = \sum_q \hbar\omega_q \hat{b}_q^\dagger \hat{b}_q$, and $\hat{H}_{\text{e-b}} = \sum_{q,\nu\eta} \langle\nu|\hat{\chi}_q|\eta\rangle \hat{b}_q \hat{c}_\nu^\dagger \hat{c}_\eta + \text{H.c.}$ Here, $\hat{h}_t$ is the single-particle system Hamiltonian, and $\hat{\chi}_q$ describes the coupling to bath mode q. The operators $\hat{c}_\alpha^\dagger$, $\hat{c}_\alpha$ ($\hat{b}_q^\dagger$, $\hat{b}_q$) create and annihilate fermions (bosons) in state $|\alpha\rangle$ (mode q). The bath is assumed to be in thermal equilibrium, with Bose-Einstein occupation $N_q = 1/(e^{\beta_T\hbar\omega_q} - 1)$ and temperature $k_B T_{\rm bath} = 1/\beta_T$. The electron system, however, can be driven far from equilibrium through the periodic drive in $\hat{H}_{\rm e}(t)$. Starting from the full quantum kinetic equation discussed in Refs. [3,5], for the system one-body density matrix, $\rho_{\nu\eta} = \langle c_\eta^\dagger c_\nu\rangle$, which contains memory effects, one can prove that in the limit of weak system-bath coupling ($\chi_q \to 0$), the steady state of this matrix has a Periodic Gibbs ensemble form [6–9]

$$\hat{\rho}_t = \sum_\alpha f_\alpha \big|\psi_\alpha^F(t)\big\rangle\big\langle\psi_\alpha^F(t)\big|, \tag{2}$$

where $|\psi_\alpha^F(t)\rangle = e^{-i\epsilon_\alpha^F t/\hbar} \sum_{n=-\infty}^{\infty} e^{-in\Omega t} |\phi_\alpha^n\rangle$ are the solutions of the time-dependent single-particle Schrödinger equation for h_t, ϵ_α^F are the Floquet energies, and $\Omega = 2\pi/T$. Hereafter, all summations over Floquet modes (for example, those labeled by n) are understood to run from $-\infty$ to ∞, and we suppress these limits for brevity. This solution reflects the synchronization of the system with the external periodic drive. The occupations of the Floquet states f_α are time independent and are obtained by solving the following Floquet-Boltzmann equation (see Appendix A of the Supplemental Material [10]),

$$\sum_\beta f_\beta \bar{f}_\alpha \big\langle W_t^{\alpha\to\beta}\big\rangle_T - \sum_\beta \bar{f}_\beta f_\alpha \big\langle W_t^{\beta\to\alpha}\big\rangle_T = 0, \tag{3}$$

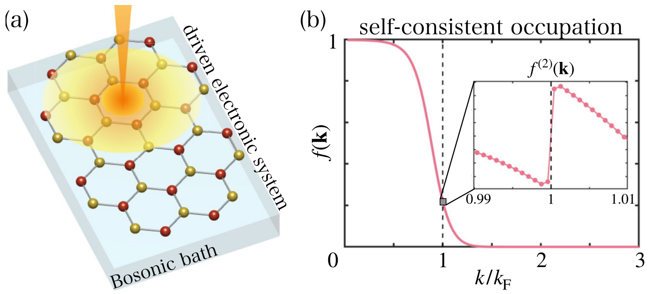

FIG. 1. (a) Strongly driven electrons coupled to an ohmic bosonic bath and irradiated by light of frequency Ω. (b) The resulting steady-state occupation develops a discontinuity in its second derivative at momentum $k_F^2/(2m) = \hbar\Omega$. Here, we choose $\bar{n}_e = n_e h/(m\Omega) = 0.8$ and $\kappa^2 = e^2|\mathcal{E}|^2/(m\hbar\Omega^3) = 0.04$.

where $\langle W_t^{\alpha\to\beta}\rangle \equiv \int_0^T (W_{e,t}^{\alpha\to\beta} + W_{a,t}^{\alpha\to\beta})dt/T$ is the time-averaged transition rate from state α to β and $\bar{f}_\alpha = 1 - f_\alpha$. The emission rate is given by

$$\langle W_{e,t}^{\alpha\to\beta}\rangle = \frac{2\pi}{\hbar}\sum_{n,q}\left|V_{\alpha\to\beta}^n(q)\right|^2\delta\left(\epsilon_\beta^F - \epsilon_\alpha^F + \hbar\omega_q + n\hbar\Omega\right),$$

$$\left|V_{\alpha\to\beta}^n(q)\right|^2 = (N_q+1)\left|\sum_m \langle\phi_\alpha^m|\hat{\chi}_q|\phi_\beta^{m+n}\rangle\right|^2, \tag{4}$$

while the absorption rate $\langle W_{a,t}^{i\to f}\rangle_T$ is obtained from Eq. (4) by substitution $N_q + 1 \to N_q$, $\omega_q \to -\omega_q$, $\hat{\chi} \to \hat{\chi}^\dagger$ [5]. The above results generalize the results of Ref. [3] to arbitrary periodically driven free-fermion Hamiltonians with an arbitrary vertex coupling to a boson bath. Similar Floquet Boltzmann equations have also been derived in Refs. [11–14]. Notice that the above scattering rates obey a generalized form of Fermi's Golden rule. This rule allows violations of Floquet energy conservation modulo Ω (Floquet umklapp). Crucially, these rates do not obey detailed balance. In the limit of vanishing amplitude of the drive, the Floquet wave function becomes static and $|\phi_{\alpha,n}\rangle \to \delta_{n0}|\phi_{\alpha,0}\rangle$, the *Floquet Fermi's Golden Rule* reduces to the standard Fermi's Golden Rule.

III. FLOQUET NON-FERMI LIQUID AT ZERO MAGNETIC FIELD

As demonstrated in Ref. [3], the steady state of Fermions driven by monochromatic light and coupled to boson baths displays emergent nonanalyticities at certain momenta which resemble the Fermi surfaces of a non-Fermi liquid. Let us review the nature of these states before generalizing to finite magnetic fields. We take a system of parabolic fermions subjected to uniform monochromatic radiation,

$$\hat{h}_t = \left[\mathbf{p} - \frac{e}{\hbar}\mathbf{A}(t)\right]^2\bigg/(2m), \tag{5}$$

where $\mathbf{A}(t) = -i\Omega^{-1}\boldsymbol{\mathcal{E}}_+\exp(-i\Omega t) + \text{c.c.}$ with $\boldsymbol{\mathcal{E}}_- = (\boldsymbol{\mathcal{E}}_+)^*$. The intensity of the light will be parametrized by the dimensionless constant $\kappa^2 = e^2|\mathcal{E}|^2/(m\hbar\Omega^3)$. The bath is taken as a collection of harmonic oscillators coupled to the on-site electron density. Namely, the boson modes in Eq. (1) are labeled as $q = (\mathbf{R}, \lambda)$, where λ counts the different oscillators at site $\mathbf{R}$. All modes are coupled with the same strength, χ_0, to the fermions, namely $\hat{\chi}_q = \chi_0|\mathbf{R}\rangle\langle\mathbf{R}|$. We take the oscillator frequencies to approach a continuum density of states (DOS) given by $\nu_B(\epsilon) \propto (\epsilon + c_2\epsilon^2)\Theta(\epsilon)$, where c_2 parametrizes the deviation from ideal ohmic bath (realized when $c_2 = 0$).

Because of translational invariance, the steady-state occupation obtained by solving Eq. (3) is a function of momentum, $f_\alpha \to f(\mathbf{k})$. As shown in Ref. [3], for an ohmic bath this steady state displays discontinuities of the second derivative of $f(\mathbf{k})$ at $\mathbf{k}_F^2/(2m) = n\hbar\Omega$ for integer n, which behave as the Fermi surface of a non-Fermi-liquid state [15]. For concreteness we will focus on the Fermi surface at $n = 1$ which is the strongest at small driving amplitudes. Notice that the effective Fermi energy is controlled by driving frequency Ω, unlike the equilibrium Fermi energy which is determined by the fermion density. Figures 2(a)–2(c) show the behavior of the second-order discontinuity $\delta f^{(2)} \equiv f''[\epsilon = \hbar\Omega + 0] - f''[\epsilon = \hbar\Omega - 0]$ for the $n = 1$ Fermi surface obtained directly from numerical solutions of Eq. (3) [see also Fig. 1(b)], corroborating the remarkable finding of Ref. [3] that these nonanalyticities remain sharp at finite bath temperature (i.e., the "ultracritical" behavior).

The strength of this emergent Fermi surface (i.e., the size of the discontinuity) is nonmonotonic as a function of the bath temperature, as shown in Figs. 2(a)–2(c). At low temperatures ($k_BT_{\text{bath}} \ll \hbar\Omega$), the strength of the emergent Fermi surface first decreases rapidly with temperature and can be fit as $\delta f^{(2)}[\tau \to 0] = (a + b\tau)e^{-\tau/c}$, where $\tau = k_BT_{\text{bath}}/\hbar\Omega$ is dimensionless temperature [see Fig. 2(c)] (for the fit parameters, see Appendix I of the Supplemental Material [10]). The size of the discontinuity in this regime saturates at large dimensionless light intensity, κ^2, at values of order $\delta f^{(2)} \sim (\hbar\Omega)^{-2}$.

Remarkably, at higher temperatures there is a revival of the strength of the emergent Fermi surface that can peak at a temperature comparable to frequency of the drive, i.e., $k_BT_{\text{bath}} \sim \kappa\hbar\Omega$ as seen in Figs. 2(b) and 2(f). Amazingly, this implies that the Fermi surface remains sharp at high temperatures comparable to the effective Fermi energy, and its decay at high temperatures can be approximated as a power law: $\delta f^{(2)}[\tau \gg \tau_{\max}] = a'\tau/(b' + \tau^2)$ [see Fig. 2(c)] (for the fit parameters, see Appendix I of the Supplemental Material [10]). Strikingly, as we will show in the next section, even such a seemingly weak nonanalyticity of the occupation gives rise to quantum oscillations comparable in magnitude to those in an ordinary Fermi liquid. The presence of this higher-temperature revival of the Fermi surface is ultimately controlled by the deviation from the perfectly ohmic bath, namely, for $c_2 \to 0$ the high-temperature revival is absent (see Appendixes I and G of the Supplemental Material [10]).

IV. KINETICS OF DRIVEN LANDAU LEVELS

We will now discuss the response of the Floquet non-Fermi liquid to a magnetic field. The electron Hamiltonian from

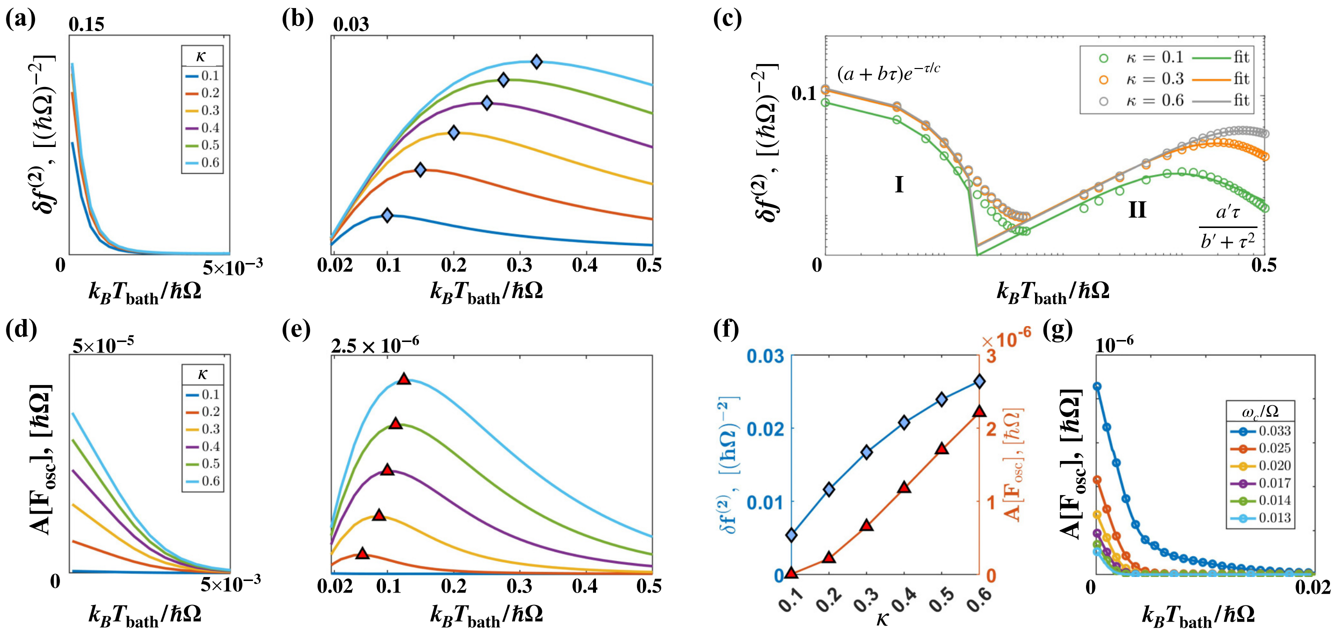

FIG. 2. Jump of the second derivative of the steady-state occupation and the resulting quantum-oscillation amplitude. Top row: temperature dependence of the jump $\delta f^{(2)}$ for $\bar{n}_e = 0.8$ and several driving amplitudes κ, shown in (a) the low-temperature regime, (b) the high-temperature regime, and (c) on a log-log scale over the full temperature range together with the fits discussed in Sec. III. Bottom row: amplitude of the resulting quantum oscillations in the interval $\Omega/\omega_c \in [40, 43]$ in (d) the low-temperature and (e) the high-temperature regimes. (f) Comparison between the jump $\delta f^{(2)}$ and the oscillation amplitude maxima as a function of driving amplitude in the high-temperature regimes. (g) Low-temperature Floquet oscillations for different magnetic fields, showing that the full width at half maximum (FWHM) scales approximately linearly with ω_c.

Eq. (5) is therefore modified to be

$$\hat{h}_t = \left[\mathbf{p} - \frac{e}{\hbar}\mathbf{A}_0(\mathbf{r}) - \frac{e}{\hbar}\mathbf{A}(t)\right]^2 \Big/ (2m), \tag{6}$$

where $\nabla \times \mathbf{A}_0(\mathbf{r}) = \mathbf{B}_0$ accounts for the constant magnetic field. Solutions to Schrödinger's equation associated with Eq. (6) have been discussed in quantum optics [19,20], and can be obtained via the unitary transformation $D[\alpha(t)] = \exp[\alpha(t)\hat{a}^\dagger - \alpha^*(t)\hat{a}]$, where $\alpha(t) = \sum_{\xi=\pm1} z_\xi e^{-i\xi\Omega t}/(\hbar\omega_c - \xi\hbar\Omega)$ with $z_\xi = -i\xi\Omega^{-1}\sqrt{\hbar\omega_c/(2m)}(\mathcal{E}^x_\xi - i\mathcal{E}^y_\xi)$, as follows (see Appendix B of the Supplemental Material [10] and Ref. [21] for more details),

$$\begin{aligned}|N, r, t\rangle &= e^{-i\Phi_N(t)} D[\alpha(t)]|N\rangle \otimes |r\rangle,\\ &= e^{-i\Phi_N(t)} \sum_{n=-\infty}^{\infty} e^{-in\Omega t}\left|\phi^n_N\right\rangle \otimes |r\rangle,\end{aligned} \tag{7}$$

where $\Phi_N(t) = E_N(t - t_0)/\hbar + (1/\hbar)\int_{t_0}^t \Delta(t')\,dt'$, $E_N = \hbar\omega_c(N + 1/2)$, N is the Landau-level index, r is the intra-Landau-level guiding center index, $\omega_c = e|\mathbf{B}_0|/m$ is the cyclotron frequency, and $\Delta(t)$ is a periodic, Landau-level-index-independent scalar energy shift generated by the displacement transformation; its explicit form is given in Appendix B of the Supplemental Material [10]. In the second line of Eq. (7) we used the Floquet theorem to express the wave function as a sum of Floquet harmonics.

Owing to magnetic translational symmetry, the scattering rates and occupations become independent of the guiding center index r (see Appendix D of the Supplemental Material [10]), allowing Eq. (4) to be recast as

$$\begin{aligned}\left\langle W^{N\to N'}_{e,t}\right\rangle_T &= \frac{2\pi}{\hbar}\sum_n \int_{-\infty}^{\infty} d\epsilon\, \nu_B(\epsilon)\left|V^n_{NN'}(\epsilon)\right|^2 \delta\left(E^n_{N'N} + \epsilon\right),\\ \left|V^n_{NN'}(\epsilon)\right|^2 &= \frac{\chi_0^2}{4\pi^2 l_B^4}(N_b(\epsilon) + 1)Q^n_{NN'},\\ Q^n_{NN'} &= \mathrm{Tr}\left\{\left[\sum_m \left|\phi^m_N\right\rangle\!\left\langle\phi^{m-n}_{N'}\right|\right]\left[\sum_{m'} \left|\phi^{m'}_N\right\rangle\!\left\langle\phi^{m'-n}_{N'}\right|\right]^\dagger\right\},\end{aligned} \tag{8}$$

where $E^n_{NN'} = E_N - E_{N'} + n\hbar\Omega$, and l_B is the magnetic length. The trace can be evaluated with the following identity,

$$\begin{aligned}Q^n_{NN'} = &\int_0^1\int_0^1 dx\,dy\, e^{i2\pi n(x-y)} e^{-|\beta(x,y)|^2}\\ &\times L_{N'}(|\beta(x,y)|^2) L_N(|\beta(x,y)|^2),\end{aligned} \tag{9}$$

where $L_N(x)$ is the Laguerre polynomial. For circularly polarized light, $|\beta(x,y)|^2 = 2\kappa^2(\omega_c/\Omega)\{1 - \cos[2\pi(x-y)]\}$ (see Appendix E of the Supplemental Material [10] for a more general form). In the limit $\kappa \to 0$, Eq. (9) vanishes for $n \neq 0$, and Eq. (3) reduces to the conventional Boltzmann equation. However, the above equations are nonperturbative and valid for any value of κ. Equipped with Eqs. (9) and (8), we numerically solve the Floquet-Boltzmann Eq. (3).

V. ULTRACRITICAL QUANTUM OSCILLATIONS

We now illustrate that the nonanalyticity of the occupation indeed behaves as the Fermi surface of a non-Fermi liquid by showing that it gives rise to quantum oscillations with markedly different behavior compared to an equilibrium Fermi liquid. Quantum oscillations are expected to appear in many observables, but for concreteness we will focus on a nonequilibrium free energy defined as

$$\frac{F}{n_e l_B^2} \equiv \frac{1}{n_e l_B^2} \sum_{N=0}^{\infty} [f_N E_N - T_{\mathrm{bath}} S_N], \tag{10}$$

where $S_N = -k_B(f_N \log f_N + \bar{f}_N \log \bar{f}_N)$ is the entropy contribution associated with the filling f_N (see Appendix C of the Supplemental Material [10]). This free energy can be obtained from the physical energy of the system averaged over one period (see Appendix C of the Supplemental Material [10] for a detailed derivation) and subtracting the entropy multiplied by the bath temperature. Therefore, this free energy is a linear combination of two physically meaningful quantities (the average energy and the entropy) chosen such that in the limit of weak driving ($\kappa \to 0$) it approaches the standard equilibrium Helmholtz free energy, which is the natural thermodynamic potential when a system is coupled to a bath with which it only exchanges energy. However, some caution should be exercised in interpreting this nonequilibrium free energy, because equilibrium relations such as those allowing to compute other physical quantities (such as heat capacity or magnetization) from its derivatives do not necessarily hold away from equilibrium.

We have evaluated Eq. (10) by numerically solving the Boltzmann Eq. (3) using scattering rates that are perturbative and nonperturbative in κ (see Appendix E of the Supplemental Material [10]), and verified that both calculations give the same behavior at small κ (see Appendix E of the Supplemental Material [10]). The perturbative rates are more efficient for numerical simulations, and we used them to explore in more detail the full temperature dependence.

Figure 3 shows that oscillations with a period associated with an effective Fermi energy $\hbar\Omega$ emerge as κ increases. These oscillations can be easily distinguished from the standard equilibrium oscillations which have a different period controlled by electron density, and which decrease as κ increases as a result of electron heating. One of our most remarkable findings, seen in Fig. 3(b), is that these new oscillations of the emergent Floquet Fermi surface remain nonanalytic as a function of *magnetic field* even when the bath is at finite temperature. This is a manifestation of their "ultracritical" nature, namely the fact that the emergent Floquet Fermi surface remains sharp at finite temperature [3]. In equilibrium quantum oscillations are nonanalytic as a function of field only at zero temperature, and happen when the chemical potential jumps across the cyclotron gaps between Landau levels, which manifests as cusplike features in the energy versus filling factor plots (i.e., inverse magnetic field) [4,22]. Therefore, what we see in Fig. 3(b) is a nonequilibrium version of this behavior that amazingly remains sharp even at finite temperatures.

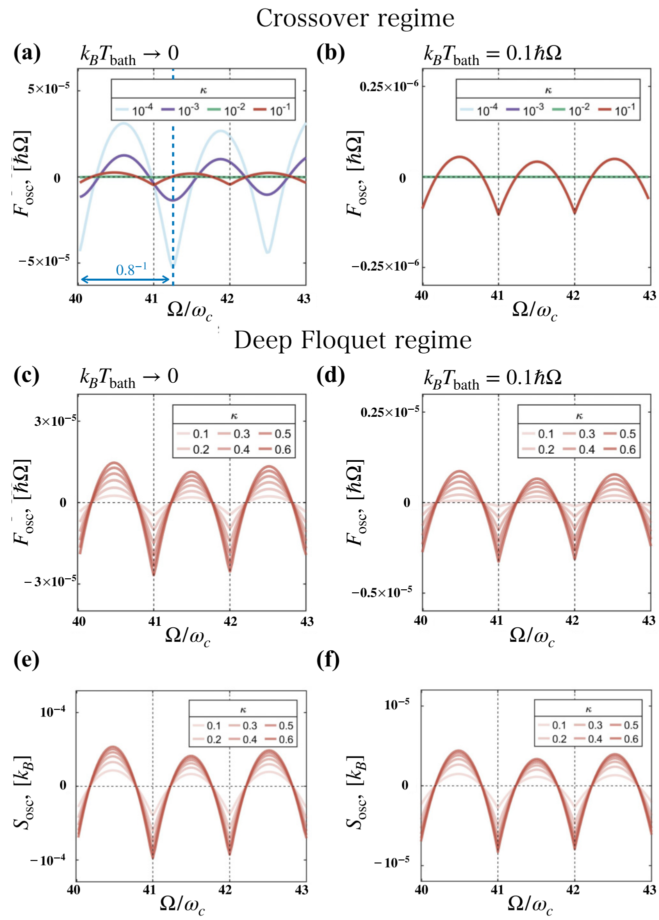

FIG. 3. (a) Quantum oscillations at small driving amplitudes κ and low bath temperature. In the limit $\kappa \to 0$, only equilibrium oscillations, controlled by the particle density, are visible; these are rapidly suppressed as κ increases, giving way to emergent Floquet oscillations with a period dictated by Ω. (b) At higher bath temperatures, equilibrium oscillations are exponentially suppressed, while Floquet oscillations remain distinct and nonanalytic as a function of magnetic field. (c), (d) At larger driving amplitudes, only Floquet quantum oscillations persist in both the low- and high-temperature regimes. (e), (f) Corresponding low- and high-temperature quantum oscillations of the von Neumann entropy.

We have also found that the amplitude is nonmonotonic as a function of temperature, as shown in Fig. 2, going first through a regime of rapid decrease with bath temperature, followed by a high-temperature revival that eventually peaks at a temperature comparable with the driving frequency $\hbar\Omega$ (i.e., the effective Floquet Fermi energy), and subsequently decaying as $\sim 1/T_{\mathrm{bath}}$ at higher temperatures. Therefore, the amplitude of oscillations is well correlated with the strength of the emergent Fermi surface, measured from the size of the jump of the second derivative at zero field, $\delta f^{(2)}$, as shown in Fig. 2.

The amplitude of the Floquet quantum oscillations at low temperatures can be comparable (see Appendix B of the Supplemental Material [10]) to the amplitude of the usual equilibrium quantum oscillations for strong light intensities $\kappa^2 \sim 1$, but it remains up to about 10% of it even down weaker intensities $\kappa^2 \sim 0.01$. On the other hand, the high-temperature oscillations tend to remain relatively weaker in amplitude than the equilibrium oscillations, i.e., for $\kappa^2 = 1$ they are about a few percent at their highest. The temperature width of the region of high-temperature oscillations is weakly dependent on magnetic field, but the temperature width of the low-temperature oscillations increases linearly with magnetic field, i.e., the latter is more similar to usual quantum oscillations [4,22]. All of the above substantiates the idea that the nonanalyticity behaves as an emergent Fermi surface, which governs the observed oscillatory behavior at small magnetic fields, and that can retain quantum features even up to remarkably elevated temperatures.

The basic mechanism underlying magnetic oscillations is that, as the magnetic field is varied, Landau levels cross the effective Floquet Fermi surfaces of the Floquet non-Fermi-liquid state, which are set by the driving frequency. Therefore, one expects oscillations not only in this free energy but also in a variety of other observables, in analogy to the equilibrium case. To illustrate this explicitly, we have also computed the von Neumann entropy of the state (see Appendix C of the Supplemental Material [10] for details) whose oscillations are shown in Figs. 3(e) and 3(f).

We caution readers that while our current calculations are very valuable as proofs of principle, there are many realistic ingredients that are crucial in order to understand the visibility in experiments of these nonequilibrium quantum oscillations that we have so far neglected, and which we hope to incorporate in future studies. One of the crucial ingredients we have neglected is the effect of Landau-level broadening. The reason we have neglected this is that our work focuses on understanding systematically the nonequilibrium steady state in the limit of weak coupling to the bath, i.e., $\hat{\chi}_{\mathbf{q}} \to 0$ in Eq. (1). Notice that the nonequilibrium occupations that solve the Boltzmann Eq. (3) are of order zero in the system bath coupling. Thus the leading effect in the limit $\hat{\chi}_{\mathbf{q}} \to 0$ is to reshuffle the occupation of states by a large amount ultimately controlled by the amplitude of the drive (but approximately independent of the strength of the coupling to the bath). At higher orders in perturbation theory, a finite coupling to the bath gives rise also self-consistently to the finite broadening Γ of the Landau levels.

A systematic account of such broadening requires a self-consistent nonequilibrium Green's function calculation, which is beyond the scope of our work. Nevertheless, we would like to comment on the broad expectations arising from accounting for this broadening (which for real experiments would also need to account not only for the coupling to the bath, but also for the effects of disorder and electron-electron interactions). In equilibrium quantum-oscillation problems, finite level broadening Γ suppresses the oscillation amplitude through the usual Dingle damping factor, e.g., $R_D = \exp[-\pi\Gamma/\omega_c]$ (see, e.g., Ref. [23]). Thus we expect that also in the present driven problem additional broadening and finite lifetime effects would reduce the oscillation amplitude and eventually wash it out once the broadening becomes comparable to the Landau-level spacing. Characterizing the impact of this broadening in a systematic fashion in the nonequilibrium setting remains an important direction for future work.

VI. GUIDING EXPERIMENTS TOWARDS TRUE FLOQUET STEADY STATES

One major open experimental challenge is to realize *true steady-state* occupations of Floquet bands and not simply short-lived transients. Currently, a large portion of Floquet experiments is performed with ultrafast optical techniques. While they have produced many beautiful results, such as the realization of Floquet states in topological insulator surfaces [24] and the light-induced Hall effect in graphene [25], these approaches only realize Floquet states for short durations (typically picoseconds), and are far from reaching true steady states, making it difficult to probe and model their behavior. Reaching such steady states would highly facilitate the observation of our nonequilibrium states with emergent Fermi surfaces, because it would allow to perform similar experiments to those employed to detect Fermi surfaces in equilibrium (e.g., quantum oscillations under magnetic fields). How can experiments reach such states? the, strength of Floquet effects is typically controlled by the work performed by the electric field during one cycle divided by the photon energy, namely by the dimensionless parameter

$$\beta_F = \frac{v\, e|\mathcal{E}|}{\hbar\,\Omega^2}, \tag{11}$$

where v is the typical electron velocity.

Floquet effects start to become visible when the dimensionless light intensity, β_F^2, is not too small. For example, for ultrafast optical approaches typically performed using midinfrared light with $\hbar\Omega \sim 120$ meV, Floquet effects can be visible when $\beta_F^2 \sim 0.1$, but this requires extremely high intensities typically of the order $10^{12}\ \mathrm{W/m^2}$. Such high intensities can lead to extreme heating of the samples, and thus are typically applied only on very short picosecond pulses (see, however, Refs. [24,26]). But notice that β_F^2 not only increases with light intensity, but also very fast as Ω^{-4} as frequency is lowered. Therefore, we believe this to be a highly promising avenue to reach Floquet states under continuous illumination because it permits to reach large values of β_F^2 at low intensities, leading to less heating and allowing the system to settle into truly quantum nonequilibrium steady states. Ultimately, Floquet effects can be washed out once the frequency becomes comparable to quasiparticle lifetime scales, and thus it is desirable to have ultraclean materials and push the frequency to be as low as possible. Are there precedents for reaching this regime? Yes, to some extent. A variety of beautiful steady-state effects have been observed in two-dimensional electron gases (2DEGs) such as GaAs heterostructures, known as microwave-induced resistance oscillation (MIRO) phenomena [23,27]. For example, in GaAs with 10 GHz only an intensity of $0.2\ \mathrm{W/m^2}$ is needed to reach $\beta_F^2 \sim 0.1$. But these investigations have largely not yet expanded to other quantum materials (e.g., only one experiment has reported related phenomena in graphene [28]).

We anticipate that interactions, by enhancing scattering processes, will lead to hotter steady states compared to the noninteracting case. Since the nonanalytic features survive at finite temperature and decay only as a power law, this additional heating should not eliminate them, although their magnitude will be reduced. More importantly, interactions generate a finite quasiparticle lifetime, an effect that lies beyond the Floquet-Boltzmann description. We expect that as long as this lifetime exceeds the Floquet period, the non-Fermi surfaces should remain observable. Clarifying this criterion, as well as the role of disorder and the minimal frequency required for their stability as true steady states, are very important questions that we hope to systematically address in future investigations.

VII. SUMMARY

We derived a Floquet-Boltzmann kinetic equation for the occupation of states in a periodically driven fermionic system coupled to an ohmic bosonic bath. We demonstrated that its solutions display nonanalyticities at certain momenta which behave as emergent Fermi surfaces, by showing that they give rise to quantum oscillations of observables in the presence of magnetic fields. These oscillations have many remarkable differences with respect to equilibrium quantum oscillations, e.g., their period is controlled by the driving frequency (not the electron density), they are nonanalytic as a function of magnetic field, nonmonotonic as a function of temperature, can survive up to extremely high temperatures comparable to the driving frequency, and their amplitude can be comparable to those in equilibrium.

ACKNOWLEDGMENTS

We would like to thank Jurgen Smet, Andrei Pimenov, Alexey Shuvaev, and Michael Zudov for stimulating discussions. We acknowledge support by the Deutsche Forschungsgemeinschaft (DFG) through Research Grant Projects No. 542614019, No. 518372354, and No. 555335098.

DATA AVAILABILITY

The data that support the findings of this article is publicly available at [29].

[1] O. Matsyshyn, J. C. W. Song, I. S. Villadiego, and L.-K. Shi, Fermi-Dirac staircase occupation of Floquet bands and current rectification inside the optical gap of metals: An exact approach, Phys. Rev. B **107**, 195135 (2023).

[2] L.-K. Shi, O. Matsyshyn, J. C. W. Song, and I. S. Villadiego, Floquet Fermi liquid, Phys. Rev. Lett. **132**, 146402 (2024).

[3] L.-K. Shi, O. Matsyshyn, J. C. W. Song, and I. S. Villadiego, Ultracritical Floquet non-Fermi liquid, Phys. Rev. Lett. **134**, 196401 (2025).

[4] D. Shoenberg, *Magnetic Oscillations in Metals*, Cambridge Monographs on Physics (Cambridge University Press, Cambridge, UK, 1984).

[5] F. T. Vasko and O. E. Raichev, *Quantum Kinetic Theory and Applications: Electrons and Photons in Semiconductors* (Springer, Berlin, 2005).

[6] A. Lazarides, A. Das, and R. Moessner, Periodic thermodynamics of isolated quantum systems, Phys. Rev. Lett. **112**, 150401 (2014).

[7] A. Lazarides, A. Das, and R. Moessner, Equilibrium states of generic quantum systems subject to periodic driving, Phys. Rev. E **90**, 012110 (2014).

[8] A. Lazarides, A. Das, and R. Moessner, Fate of many-body localization under periodic driving, Phys. Rev. Lett. **115**, 030402 (2015).

[9] V. Khemani, A. Lazarides, R. Moessner, and S. L. Sondhi, Phase structure of driven quantum systems, Phys. Rev. Lett. **116**, 250401 (2016).

[10] See Supplemental Material at http://link.aps.org/supplemental/10.1103/pmsn-5jtp for additional details on the derivation of the Floquet-Boltzmann equation, the driven Landau-level solution, scattering amplitudes, the effective cycle-averaged free energy and entropy, numerical procedures, and fitting parameters.

[11] K. I. Seetharam, C.-E. Bardyn, N. H. Lindner, M. S. Rudner, and G. Refael, Controlled population of Floquet-Bloch states via coupling to Bose and Fermi baths, Phys. Rev. X **5**, 041050 (2015).

[12] M. Genske and A. Rosch, Floquet-Boltzmann equation for periodically driven Fermi systems, Phys. Rev. A **92**, 062108 (2015).

[13] I. Esin, M. S. Rudner, G. Refael, and N. H. Lindner, Quantized transport and steady states of Floquet topological insulators, Phys. Rev. B **97**, 245401 (2018).

[14] K. I. Seetharam, C.-E. Bardyn, N. H. Lindner, M. S. Rudner, and G. Refael, Steady states of interacting Floquet insulators, Phys. Rev. B **99**, 014307 (2019).

[15] This "non-fermi-liquid" behavior originates ultimately from the nontrivial occupation of states which arise even at weak coupling in nonequilibrium steady states due to the lack of detailed balance. we caution that this is a distinct phenomenon that should not be confused with non-fermi-liquid behavior in equilibrium [16–18].

[16] T. Giamarchi, *Quantum Physics in One Dimension*, International Series of Monographs on Physics (Clarendon Press, Oxford, UK, 2003), Vol. 121.

[17] T. Senthil, Critical Fermi surfaces and non-Fermi liquid metals, Phys. Rev. B **78**, 035103 (2008).

[18] C. M. Varma, Z. Nussinov, and W. van Saarloos, Singular or non-Fermi liquids, Phys. Rep. **361**, 267 (2002).

[19] S. M. Roy and V. Singh, Generalized coherent states and the uncertainty principle, Phys. Rev. D **25**, 3413 (1982).

[20] C. Gerry and P. Knight, *Introductory Quantum Optics* (Cambridge University Press, Cambridge, UK, 2004).

[21] L.-K. Shi, Algebraic exact solution for driven Landau levels in two-dimensional electron gases, Phys. Rev. B **112**, 165108 (2025).

[22] A. A. Abrikosov, *Fundamentals of the Theory of Metals* (Courier Dover Publications, Mineola, NY, 2017).

[23] I. A. Dmitriev, A. D. Mirlin, D. G. Polyakov, and M. A. Zudov, Nonequilibrium phenomena in high Landau levels, Rev. Mod. Phys. **84**, 1709 (2012).

[24] Y. H. Wang, H. Steinberg, P. Jarillo-Herrero, and N. Gedik, Observation of Floquet-Bloch states on the surface of a topological insulator, Science **342**, 453 (2013).

[25] J. W. McIver, B. Schulte, F.-U. Stein, T. Matsuyama, G. Jotzu, G. Meier, and A. Cavalleri, Light-induced anomalous Hall effect in graphene, Nat. Phys. **16**, 38 (2020).

[26] Y. Liu, C. Yang, G. Gaertner, J. Huckabee, A. V. Suslov, G. Refael, F. Nathan, C. Lewandowski, L. E. F. F. Torres, I. Esin, P. Barbara, and N. G. Kalugin, Signatures of Floquet electronic steady states in graphene under continuous-wave mid-infrared irradiation, Nat. Commun. **16**, 2057 (2025).

[27] Q. Shi, P. D. Martin, A. T. Hatke, M. A. Zudov, J. D. Watson, G. C. Gardner, M. J. Manfra, L. N. Pfeiffer, and K. W. West, Shubnikov–de Haas oscillations in a two-dimensional electron gas under subterahertz radiation, Phys. Rev. B **92**, 081405(R) (2015).

[28] E. Mönch, D. A. Bandurin, I. A. Dmitriev, I. Y. Phinney, I. Yahniuk, T. Taniguchi, K. Watanabe, P. Jarillo-Herrero, and S. D. Ganichev, Observation of terahertz-induced magnetooscillations in graphene, Nano Lett. **20**, 5943 (2020).

[29] O. Matsyshyn, Data for “High-temperature quantum oscillations of a nonequilibrium non-Fermi liquid” [Dataset], Zenodo, 2026, https://doi.org/10.5281/zenodo.21483630.